

available at [www.sciencedirect.com](http://www.sciencedirect.com)journal homepage: [www.ejconline.com](http://www.ejconline.com)

# Identification of a novel, functional role for S100A13 in invasive lung cancer cell lines

A. Pierce<sup>a</sup>, N. Barron<sup>\*,a</sup>, R. Linehan, E. Ryan, L. O'Driscoll, C. Daly, M. Clynes

National Institute for Cellular Biotechnology, Dublin City University, Glasnevin, Dublin 9, Ireland

## ARTICLE INFO

### Article history:

Received 10 July 2007

Received in revised form

28 September 2007

Accepted 9 October 2007

### Keywords:

Expression profiling

Invasion/metastasis

Lung cancer

## ABSTRACT

The S100 family is a group of small, calcium-binding proteins with at least 20 distinct members in humans. Several of these have been associated with cancer invasion or metastasis in recent studies. Transcriptional analysis of gene expression in a panel of lung cancer-derived cell lines identified S100A13 as being associated with a more aggressive invasive phenotype *in vitro*. Hierarchical clustering grouped this gene with several others that have established functional roles in this phenotype both *in vitro* and *in vivo* (ICAM1, CD34, EFNB2 and HGF) as well as genes involved in processes such as angiogenesis (TEM7, JAG2).

Depletion of cellular S100A13 mRNA levels by RNAi in highly invasive lung cancer cell lines resulted in a 50–80% decrease in their invasive potential in an *in vitro* assay. This reduction could not be accounted for by reduced cellular proliferation. Conversely, transient overexpression of exogenous S100A13 in less invasive cell lines had no impact on invasive potential suggesting that upregulation of S100A13 expression alone is insufficient to induce the phenotype. We conclude that S100A13 is involved in but not capable of inducing invasion, since elevated S100A13 mRNA expression correlates with a more invasive phenotype and *in vitro* invasion can be inhibited by reduced S100A13 expression.

© 2007 Elsevier Ltd. All rights reserved.

## 1. Introduction

S100 proteins are low molecular weight proteins of variable length and sequence that are expressed in a tissue-specific manner in vertebrates. To date, at least 25 S100 family members have been reported ranging in size from 9 to 13 kDa.<sup>1</sup> The S100 protein family is characterised by the presence of two distinct helix–loop–helix calcium binding motifs termed EF-hands, which are connected by a hinge region. The EF-hand at the N-terminal has a weaker affinity for Ca<sup>2+</sup> binding than its C-terminal counterpart and is sometimes referred to as a 'pseudo EF-hand'. The C-terminal EF-hand contains a more conserved EF-hand domain which has a Ca<sup>2+</sup> binding affinity 100-times greater than the N-terminal site.<sup>2–4</sup> Ca<sup>2+</sup> binding is thought to be important for the functional activity of S100

proteins, with binding inducing a conformational change in the peptides. The Ca<sup>2+</sup>-induced conformational change exposes a hydrophobic cleft between the hinge region and the classical, C-terminal EF-hand domain. This exposed hydrophobic surface represents the site at which S100 peptides interact with their target proteins. S100 proteins are generally found as homo- and heterodimers in solution. Indeed S100-multimers are thought to be required for their extracellular activity as polymeric forms of S100 proteins trigger aggregation of the RAGE receptor and thus activate intracellular signalling cascades.<sup>4</sup>

The S100 protein family has been implicated in a number of biological functions including cell division, motility, secretion, protein synthesis and membrane permeability.<sup>5–7</sup> In addition, recent studies have reported associations between

\* Corresponding author. Tel.: +353 17005804; fax: +353 17005484.

E-mail address: [niall.barron@dcu.ie](mailto:niall.barron@dcu.ie) (N. Barron).

<sup>a</sup> Both authors contributed equally to this work.

0959-8049/\$ - see front matter © 2007 Elsevier Ltd. All rights reserved.

doi:10.1016/j.ejca.2007.10.017

S100 family members and tumour development and progression, since they have altered expression levels in cancer cells compared to normal cells.<sup>8–11</sup> In particular, S100A4, S100A6, S100A7 and S100A10 have been found to correlate with, and indeed, functionally effect a more aggressive cancer phenotype.<sup>8,12–14</sup> Furthermore, Saleem and colleagues,<sup>15</sup> demonstrated that S100A4 is overexpressed during prostate cancer progression. However, the mode of action of many S100 proteins in cancer remains to be elucidated and the functional implications of altered S100 expression levels determined.

Wicki and colleagues<sup>16</sup> identified a new S100 member, termed S100A13, by screening EST databases. The C-terminus of the S100A13 protein ends with the motif RKK, which is also seen in the metastasis-associated proteins S100A4 and S100A10. Although S100A13 is similar to most S100 family members in that its homodimers possess two high- and low-affinity  $\text{Ca}^{2+}$  binding sites, it does not exhibit a calcium-dependent exposure of the hydrophobic surface which is important for the interaction of other S100 proteins with their target peptides.<sup>17</sup> This protein has since been found to play a crucial role in the release of FGF-1.<sup>18</sup> The FGF family is known to be involved in angiogenesis<sup>19</sup> and tumour metastasis and the growth is dependent upon tumour angiogenesis *in vivo*.<sup>20</sup> Indeed, it is possible that S100 gene family members, including S100A13, support neoplastic and pro-inflammatory situations *in vivo* by their ability to participate in the release pathway for angiogenic and inflammatory signals such as FGF-1 and IL-1 $\alpha$ .<sup>18,21</sup> S100A13 is widely expressed in many types of tissues, with particularly high expression in the thyroid gland. The localisation of S100A13 expression in human smooth muscle cells differs from that of all other S100 proteins. S100A13 is expressed in the perinuclear area of these cells, which suggests diverse functions for S100A13 in signal transduction.<sup>17</sup>

Recently, we performed differential transcriptional analysis of a panel of lung cancer cell line variants with differing invasive phenotypes in an *in vitro* invasion assay. An increase in S100A13 transcript was found to be associated with a more aggressive invasive phenotype and clustered with several other well-documented cancer/metastasis-related genes. As this gene had not previously been functionally linked with this phenotype, we sought to investigate any role it might play in invasion. To this end, we examined the effect of altered S100A13 expression on both proliferation and invasion in cell lines with varying invasive phenotypes.

## 2. Materials and methods

### 2.1. Cell culture

DLKP cell line variants were maintained in ATCC media (Hams F12/DMEM (1:1)) supplemented with 5%(v/v) FCS at 37 °C.

### 2.2. S100A13 siRNA transfection

siRNAs targeting S100A13 (Ambion ID 42125, 263271 and 263272) were transfected into the invasive cell lines using 2  $\mu\text{l}$  NeoFx (Ambion, TX, 4511) with 30 nM siRNA. 100  $\mu\text{l}$  of the siRNA/NeoFX/Optimem™ solution was added into each

well of a 6-well plate. Cell suspension (1 ml) was added to each well at a concentration of  $3 \times 10^5$  cells/ml. The plates were incubated at 37 °C for 24 h and then re-fed with fresh medium.

### 2.3. S100A13 cDNA transfection

S100A13 cDNA was obtained from Open Biosystems (MHS1011-59294), sub-cloned into pSPORT6 mammalian expression vector and sequenced. Transient cDNA transfection experiments were performed with 5  $\mu\text{l}$  Lipofectamine 2000 (Invitrogen, 11668019) and 2  $\mu\text{g}$  plasmid in a cell density of  $4 \times 10^5$  per well of a 6-well plate. Medium was removed after 24 h and replaced with fresh growth medium.

### 2.4. In vitro invasion assay

Invasion assays were performed using commercial invasion assay kits (Beckton Dickinson, Cat no. 354480). The invasion assay kits were allowed to come to room temperature, were rehydrated on the top and bottom of the insert with 0.5 ml pre-warmed serum-free media for 2 h at 37 °C. Following this incubation, the media underneath the insert were replaced with pre-warmed media containing 5%(v/v) FCS. 72 h following siRNA/cDNA transfection, the cells were trypsinised, counted and resuspended in pre-warmed media containing 1%(v/v) FCS at a density of  $1 \times 10^6$  cells/ml. Cell (100  $\mu\text{l}$ ) suspension was added to each insert. The cells were incubated at 37 °C for 24 h. After this, the insert was stained with 0.25%(w/v) crystal violet for 10 min, rinsed and allowed to air dry. The inserts were then viewed under the microscope and photographed. The number of invasive cells was determined by counting 10 random fields at 20 $\times$  magnification.

### 2.5. Proliferation assay

Cell number was assessed 72 h post siRNA/cDNA transfection using the acid phosphatase method. Cells were incubated with freshly prepared phosphatase substrate (10 mM *p*-nitrophenol phosphate (Sigma 104-0) in 0.1 M sodium acetate (Sigma, S8625), 0.1%(v/v) Triton X-100 (BDH, 30632), pH 5.5) in the dark at 37 °C for 2 h. The reaction was stopped by the addition NaOH and plates were read in a dual beam plate reader at 405 nm with a reference wavelength of 620 nm.

### 2.6. Quantitative and semi-quantitative RT-PCR

Total RNA was extracted using RNeasy mini kit (Qiagen, 74104). Reverse transcription reactions typically contained 1  $\mu\text{g}$  total RNA, oligo-dT, RNasin, dNTPs, and 200 U of MMLV-Reverse Transcriptase for 1 h at 37 °C. For semi-quantitative PCR, 100 ng cDNA was used as template with the following S100A13-specific primers: 5'-taatggcagcagaaccactg-3' (fwd) and 5'-ttgagctccgagtcctgatt-3' (rev). Thermocycling conditions were: 5 min at 95 °C  $\times$  1, [30 s at 94 °C, 30 s at 55 °C, 30 s at 72 °C]  $\times$  35, 5 min at 72 °C  $\times$  1. PCR products were separated on 2 % (w/v) agarose with an expected product size of 219 bp.  $\beta$ -Actin was used as the endogenous control.

Quantitative PCR (qPCR) was performed on an ABI7500 instrument (Applied Biosystems). 2.5  $\mu\text{l}$  of RT reaction was

used as template in a total of 25  $\mu$ l with Taqman™ 2 $\times$  Master-mix (Applied Biosystems, 4318157). S100A13 was amplified and detected by the addition of pre-designed 'Assay-on-Demand' primer/probe mix with FAM as reporter (Applied Biosystems, Hs00195583\_m1).  $\beta$ -Actin was used for normalisation with VIC as the reporter dye (Assay-on-Demand, Applied Biosystems, 4326315E). After activation of the DNA polymerase at 95 °C for 10 min, the target transcripts were amplified for 40 cycles of: 15 s at 95 °C and 1 min at 60 °C. Relative quantification was determined using the  $\Delta\Delta$ Ct method.

## 2.7. Western blotting

Cells were scraped directly on culture dishes using NP40 lysis buffer (20 mM Tris, pH 7.4, 50 mM NaCl, 50 mM NaF, 1%(v/v) NP40) supplemented with 1 mM PMSF, 1 mM protease inhibitor cocktail (Roche, 1,873,580) and 1 mM  $\text{Na}_3\text{VO}_4$  for 20 min on ice. Following centrifugation, equal amounts of protein (100  $\mu$ g/lane) were separated on sodium dodecyl sulphate-polyacrylamide gels (SDS-PAGE) and electroblotted onto nitrocellulose membranes. The membrane was blocked with fresh filtered 5%(w/v) non-fat dried milk (Marvel™ skimmed milk) in TBS (20 mM Tris, 0.15 M NaCl)/0.1% Tween 20 (Sigma, P1379), pH 7.4 for 2 h. After blocking, the membranes were rinsed with TBS/0.1%(v/v) Tween and incubated with rabbit anti-human S100A13 antibody (1:500) overnight at 4 °C. The primary antibody was removed and the membranes were rinsed thrice with TBS/0.1 % (v/v) Tween. The membranes

were incubated in 1:1000 dilution of HRP-labelled goat anti-Rabbit (DakoCytomation, P0448) antibody in 1%(w/v) Marvel™ for 1 h at room temperature. The secondary antibody was then removed and blots were washed three times for 15 min in TBS/0.1%(v/v) Tween. Bound antibody was detected using enhanced chemiluminescence (ECL).

## 3. Results

### 3.1. S100A13 is upregulated in invasive lung cancer cell lines

Transcriptional profiling of a panel of invasive lung cancer cell lines was performed in our laboratory using U133A Human Genome Chips (Affymetrix) to identify differentially expressed genes. The cell lines profiled were variants of the poorly differentiated human lung, squamous cell line, DLKP.<sup>22</sup> These cell lines had differing levels of invasiveness, but were derived from the same parent offering a unique opportunity to study the less-well characterised mechanisms of invasion. Two invasive, non-drug exposed, variants of the DLKP cell line (KP1, KP2) were used in the study along with a non-invasive, vincristine-resistant (VCR) variant, an invasive taxotere-resistant DLKP variant (TX2) and a non-invasive taxotere-resistant line (TX1). These variants displayed different degrees of invasiveness when assayed in an *in vitro* matrigel invasion assay ranging from non/weakly invasive to strongly invasive. The cells were assigned a numerical value denoting their relative

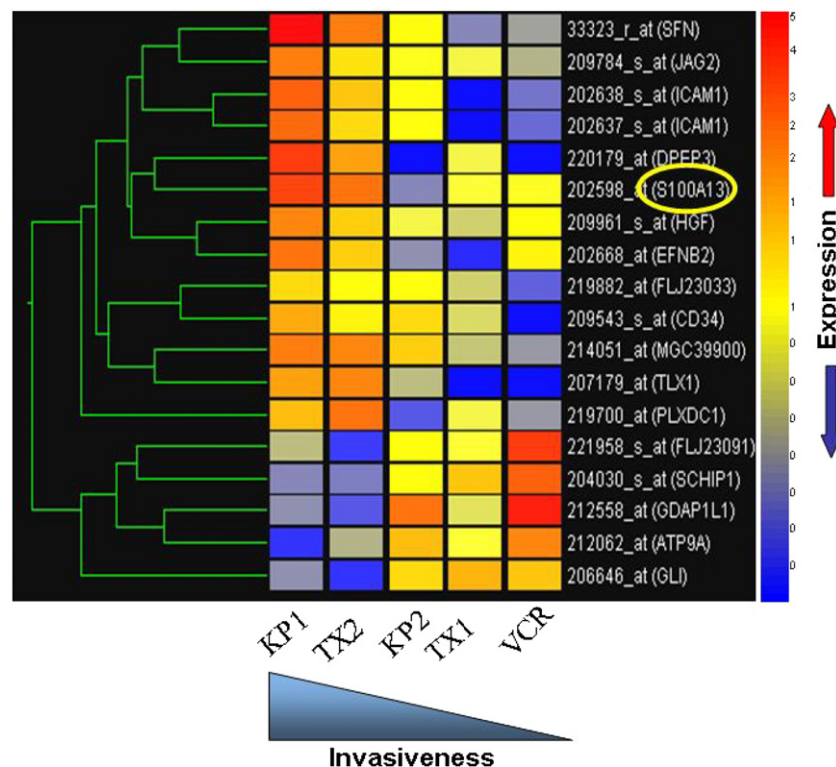


Fig. 1 – Hierarchical clustering of genes differentially expressed across a panel of lung cancer cell line variants with different invasiveness *in vitro*. Cell lines are listed by decreasing invasiveness (L–R). Gene expression patterns grouped by Pearson correlation. Red: Increased expression above median; Blue: decreased expression below median.

invasiveness as follows: VCR (0) < TX1 (1) < KP2 (3.5) < TX2 (5) = KP1 (5), where VCR is the least and TX2 and KP1 are the most invasive. This scale was applied to reflect the intermediate degrees of the phenotype in an attempt to gain insight into the more subtle transcriptional changes associated with this transition.

In the analysis, a Welch ANOVA statistical test (>2-fold up or down,  $p < 0.05$ ) was used to find genes that were differentially expressed between the five different cell lines. Subsequently, a Welch t-test was used to find genes in this list

that were useful in discriminating between more invasive (VCR, TX1) and less invasive (KP1, TX2 and KP2) samples. This generated a gene list containing 45 genes, a subset of which is illustrated in Fig. 1. In this dendrogram, the cell line clusters (Pearson correlation) are shown along the horizontal with decreasing invasiveness from left to right. It is noteworthy that there is a visible distinction between the 2 most invasive and the 2 least invasive cell line variants but that the KP2 variant seems to straddle both cohorts, in this cluster at least. Within this cluster, we identified several genes that have been

**Table 1 – Biological function (if known) of genes in cluster and fold-change expressed relative to the level detected in the least/non-invasive cell line, VCR**

| Gene ID         | Gene name  | Function   | Fold change |      |      |      |     |
|-----------------|--|--|-------------|------|------|------|-----|
|                 |  |  | KP1         | TX2  | KP2  | TX1  | VCR |
| SFN             | Stratifin  | Regulation of progression through cell cycle/// apoptotic program/// negative regulation of caspase activity   | 11.4        | 4.2  | 1.8  | 0.9  | 1   |
| JAG2            | Jagged 2   | Cell fate determination/// cell cycle/// cell cycle /// cell communication/// Notch signalling pathway/// regulation of cell migration   | 3.7         | 2.2  | 1.5  | 1.5  | 1   |
| ICAM1           | Intercellular adhesion molecule 1                              | Cell adhesion/// cell–cell adhesion/// regulation of cell adhesion   | 6.2         | 3.7  | 2.3  | 0.3  | 1   |
| DPEP3           | Dipeptidase3   | Proteolysis  | 25.7        | 13.3 | 0.9  | 5.9  | 1   |
| S100A13         | S100 A13   | cell differentiation, calcium ion binding  | 3.8         | 2.8  | 0.6  | 0.9  | 1   |
| HGF             | Hepatocyte growth factor                                       | Epithelial to mesenchymal transition/// proteolysis/// mitosis/// blood coagulation  | 2.1         | 1.3  | 0.7  | 0.7  | 1   |
| EFNB2           | Ephrin-B2  | Cell–cell signalling/// multicellular organismal development/// nervous system development/// anatomical structure morphogenesis/// cell differentiation   | 2.3         | 1.5  | 0.5  | 0.2  | 1   |
| FLJ23033        | Tubulin tyrosine ligase-like family, member 7                  | Protein modification process   | 3.2         | 2.6  | 2.3  | 1.7  | 1   |
| CD34            | Cd34 antigen   | Cell adhesion/// cell–cell adhesion/// leukocyte migration   | 31.1        | 21.1 | 22.8 | 12.2 | 1   |
| MGC39900        | Hypothetical protein MGC39900                                  | Cytoskeleton organisation and biogenesis, actin binding  | 4.3         | 4.2  | 2.7  | 1.2  | 1   |
| TLX1            | T-cell leukaemia, homeobox 1                                   | Regulation of transcription, DNA-dependent/// multicellular organismal development/// central nervous system development/// positive regulation of cell proliferation /// neuron differentiation/// cell fate commitment///  | 15.6        | 20.1 | 6.9  | 0.5  | 1   |
| PLXDC1          | Plexin domain containing 1                                     | Angiogenesis/// multicellular organismal development   | 2.8         | 4.6  | 0.7  | 1.6  | 1   |
| FLJ23091        | G protein-coupled receptor 177                                 | Transcription/// regulation of transcription, DNA-dependent/// positive regulation of I-kappaB kinase/NF-kappaB cascade  | 0.2         | 0.1  | 0.3  | 0.2  | 1   |
| SCHIP1          | Schwannomin interacting protein 1                              | Unknown  | 0.2         | 0.2  | 0.4  | 0.5  | 1   |
| GDAP1L1 (SPRY1) | Sprouty homologue 1, antagonist of FGF signalling (Drosophila) | Ureteric bud development/// induction of an organ/// multicellular organismal development/// regulation of signal transduction/// negative regulation of MAPK activity   | 0.1         | 0.3  | 0.7  | 0.4  | 1   |
| ATP9A           | ATPase, Class II, type 9A                                      | Transport/// cation transport/// metabolic process/// phospholipid transport   | 0.1         | 0.1  | 0.6  | 0.2  | 1   |
| GLI             | Glioma-associated oncogene homologue 1                         | positive regulation of cell proliferation/// cell differentiation/// lung development/// osteoblast differentiation/// transcription/// regulation of transcription, DNA-dependent/// multicellular organismal development /// spermatogenesis/// ventral midline development/// | 0.3         | 0.2  | 0.9  | 1.1  | 1   |



previously associated with cancer and, in particular, invasion or metastasis (Table 1). Of the 12 genes upregulated in more invasive cells, several had been reported previously to display dysregulated expression in cancer and/or metastases (ICAM1, CD34, HGF and SFN). Interestingly, SPRY1, an antagonist of FGF signalling, was found to be downregulated across the panel. S100A13 also appeared in this cluster. To confirm the differential expression of the S100A13 transcript in the cell line panel, we performed semi-quantitative RT-PCR. Fig. 2 confirms that the mRNA was increased by up to threefold in the more invasive compared to the less invasive cell lines. Interestingly, the level of transcript in the KP2 variant was under-estimated in the microarray analysis compared to RT-PCR.

### 3.2. Transient transfection with target-specific siRNA reduces cellular levels of S100A13 transcript

Having established that S100A13 transcript levels correlate with a more invasive phenotype, S100A13 mRNA was knocked down in an attempt to identify a possible functional role for the protein. Three independent siRNA sequences were transiently transfected into the more invasive cell line, TX2, and target mRNA depletion was monitored over a 72 h period by quantitative RT-PCR. It was important to ensure that S100A13 was suppressed at 72 h to minimise non-specific effects of the transfection procedure in the subsequent invasion assay. Not unexpectedly, measuring the invasive ability of cells that have been recently exposed to transfection reagent will impact greatly on this phenotype. We found 72 h to be the minimum recovery time required by transfected cells before being transferred to invasion chambers. As demonstrated in Fig. 3A, transient transfection with three independent siRNAs resulted in S100A13-knockdown of between 60% and 80% in TX2 cells over this timeframe. Two of the siR-

NAs maintained significant levels of knockdown up to 72 h with the third less effective at this stage. These oligonucleotides were equally effective in all three invasive cell variants over this period (Fig. 3B).

### 3.3. Knockdown of S100A13 in invasive lung cancer cell lines reduces their *in vitro* invasiveness

Cell lines KP1, KP2 and TX2 were transiently transfected with S100A13-specific siRNA and scrambled control oligonucleotides and allowed to recover for 72 h. The cells were then assayed for their ability to migrate through Matrigel™ in a chamber-based *in vitro* invasion assay (Boyden chamber). After 24 h, the inserts were stained and invading cells counted. A decrease in invasion ranging from 50% to 80% ( $p < 0.001$ ) was achieved in cell lines that were depleted in S100A13 compared to the scrambled siRNA controls (Fig. 4). The pattern of reduction correlated with the level of transcript knockdown obtained with each siRNA. It is worth noting the impact of the treatment itself on the phenotype (no treatment versus scrambled siRNA) hence the long recovery time before performing the functional assay.

### 3.4. Reduced invasiveness is not a result of decreased cellular proliferation

It was unclear at this point whether the observed reduction in invasion was merely a by-product of decreased cellular proliferation or a direct impact on cellular invasiveness. The effect of transfecting S100A13 siRNA sequences on proliferation was investigated. Cells were seeded at the cell number used to seed all the siRNA transfections. Relative cell number was determined using the acid phosphatase assay at the end of the 72 h recovery period. The treatment was found to have no impact on cell number in S100A13 depleted cells (Fig. 5) compared to the scrambled siRNA control cultures.

### 3.5. Transient overexpression of exogenous S100A13 is insufficient to induce an invasive phenotype

Having established that specific downregulation of the S100A13 gene transcript in invasive lung cancer cell variants reduces this phenotype by as much as 80%, we wished to investigate the importance of this factor in its development. Clearly many genes are differentially expressed in cells with different degrees of invasiveness but it would be useful to identify the control molecules that set the process in motion. We transfected the weakly invasive variants, TX1 and VCR, with an expression vector containing the S100A13 coding sequence driven by a strong viral promoter. High levels of expression of the exogenous protein were achieved up to 72 h post-transfection (Fig. 6). Levels of endogenous S100A13 protein expression in TX1 and VCR are below the level of detection with the antibody used here. However, this was not unexpected since S100A13 mRNA expression was lower in these less invasive variants than their invasive counterparts (Figs. 1 and 2). Despite increased S100A13 protein expression at 72 h post-transfection, invasion was not increased in TX1 and VCR cells overexpressing S100A13 compared to vector only controls (Fig. 6).

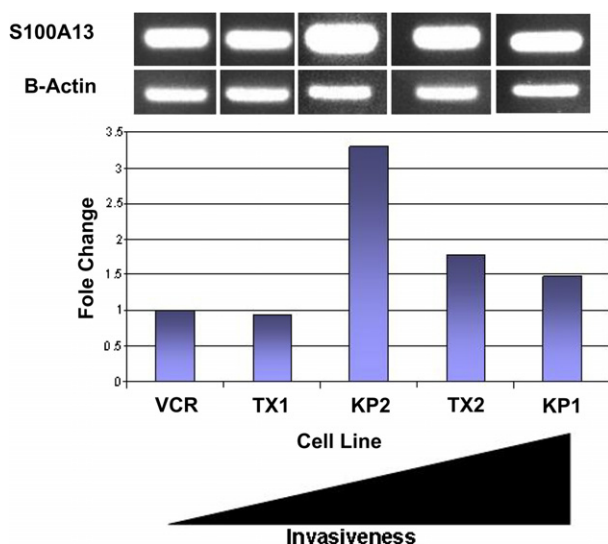


**Fig. 2 – S100A13 expression levels in a panel of DLKP variant cell lines. Semi-quantitative RT-PCR was performed as described and fold-change, relative to VCR sample, estimated by gel densitometry.**

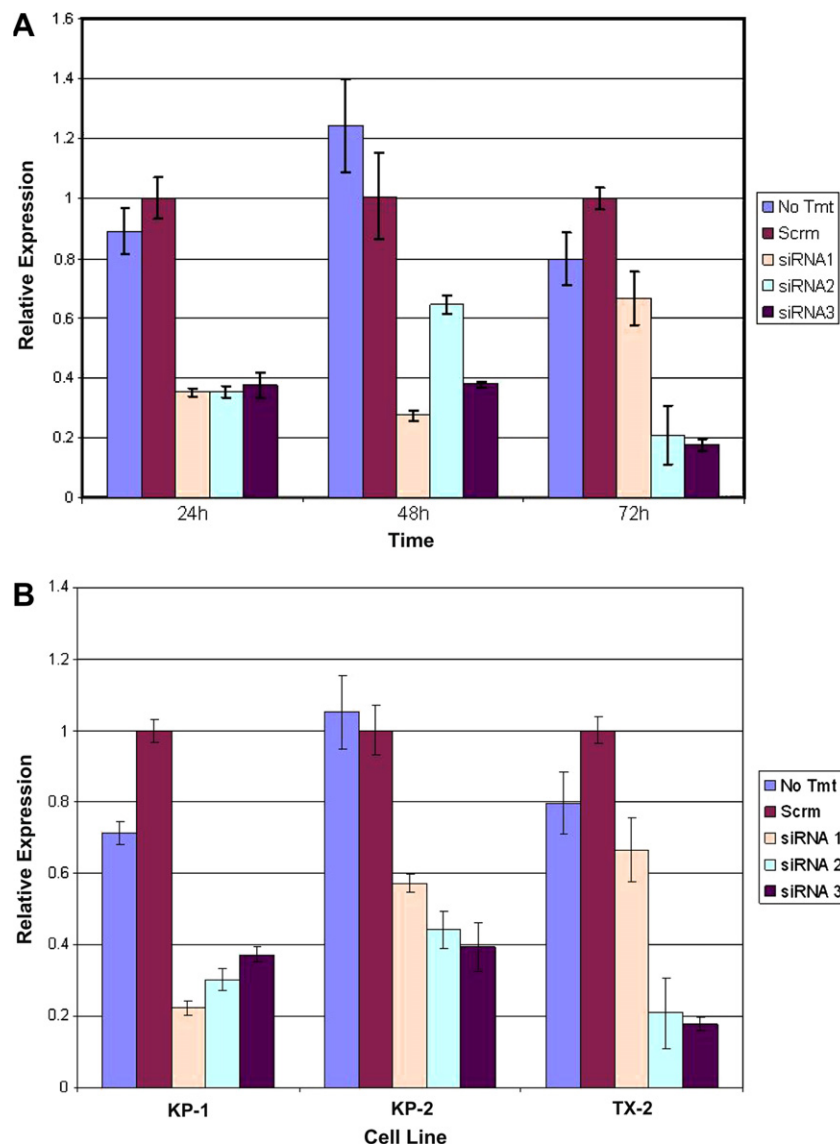


**Fig. 3 – Knockdown of S100A13 expression with three independent siRNA sequences. S100A13 expression was determined by qPCR at various sample time-points post-transfection in TX-2 (A). S100A13 expression at 72 h in the three most invasive cell lines at 72 h (B).**

#### 4. Discussion

S100 family members have been identified as molecular markers for metastatic potential.<sup>23–27</sup> For example, S100A6 expression has been associated with human colorectal adenocarcinoma tumorigenesis and metastasis and a positive correlation has been demonstrated between S100A13 expression, tumour grade and microvessel density in human astrocytic gliomas.<sup>26</sup> Invasion is an important step in the metastatic process.<sup>28</sup> Our array data indicated that S100A13 expression was increased in the more invasive variants in a panel of lung cancer cell lines which differ in their capacity to invade *in vitro* (Fig. 1). Analysis of S100A13 mRNA by RT-PCR confirmed increased expression in the invasive cell lines KP2 and TX2 compared with the weakly invasive cell lines TX1 and VCR (Fig. 2). This also served to validate the microarray-derived data. Worth noting is the apparent difference in

mRNA content in cell line KP2 as measured by microarray compared to RT-PCR. This variation is seen occasionally when validating microarray data in our experience and is most likely a result of the semi-quantitative nature of the RT-PCR method. This increase in expression concurs with a study by Smirnov and colleagues, who identified S100A13 as a novel predictor of metastasis following its detection in circulating tumour cells in blood from patients with metastatic cancer.<sup>29</sup> This may prove to be an important finding since Cristofanilli and colleagues<sup>30</sup> reported that the presence of circulating tumour cells in blood was associated with poor prognosis in patients with metastatic breast cancer.

To help define the potential role of S100A13 in invasive lung cancer, we transfected three independent S100A13 siRNA sequences in the invasive cell lines KP1, KP2 and TX2 and examined the effect of this decrease in S100A13 expression on both proliferation and invasion. An S100A13 siRNA-

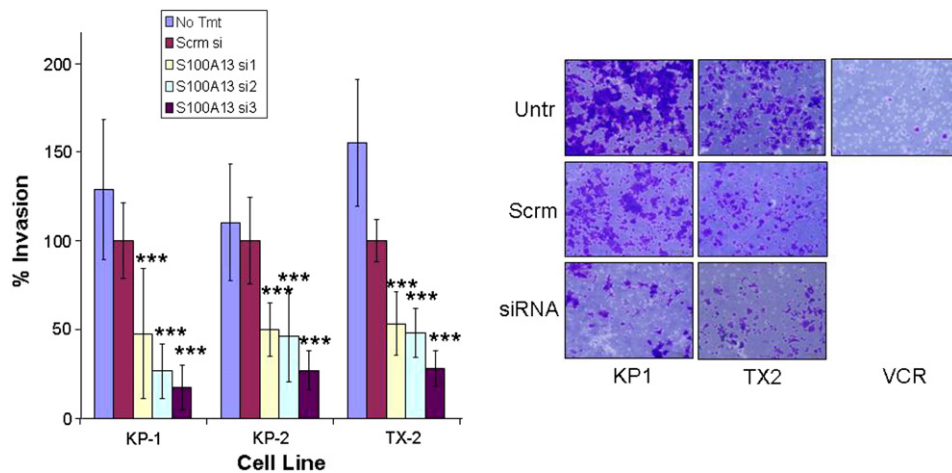


**Fig. 4** – The invasive cell lines KP-1, KP-2 and TX-2 were transfected with scrambled siRNA and three independent siRNA sequences to S100A13. The effect of S100A13 expression knockdown on invasion was examined 72 h post transfection. Ten random fields were counted per insert at 20 $\times$ . Each condition was examined using at least two invasion kit inserts. Pictures are representative fields of view. VCR are included for comparison. Counts per insert were averaged and plotted as ‘% Invasion’ after normalisation to the scrambled siRNA for each cell line ( $P < 0.001$ ).

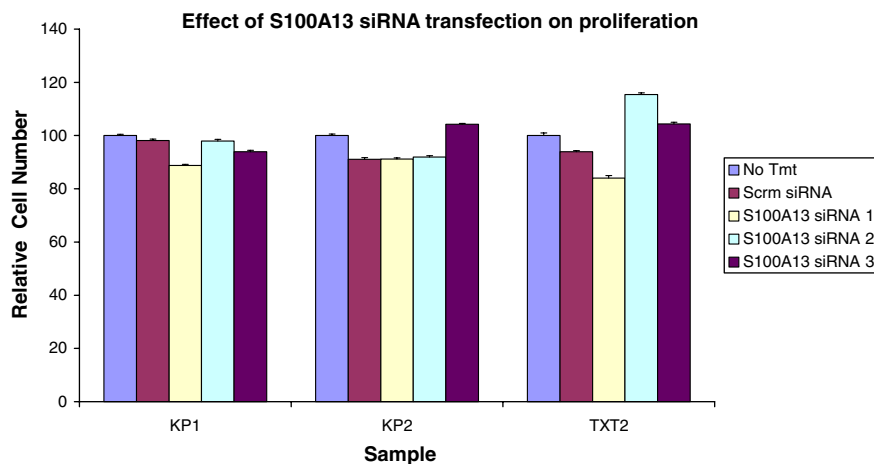


**Fig. 5** – Effect of transfecting invasive DLKP cell lines with three independent S100A13-specific siRNAs on proliferation. Cell numbers were estimated 72 h post-transfection by the acid phosphatase method and reported relative to untransfected cells.

specific decrease in mRNA levels was confirmed by qPCR analysis (Fig. 3), reflecting a corresponding decrease in invasiveness (Fig. 4). Our results show that decreasing S100A13 expression in invasive cell lines can reduce their invasive capacity by 50–80% ( $p < 0.001$ ). This is the first study to provide functional evidence for the role of S100A13 in invasion and indicates that S100A13 is potentially involved in two steps of the metastatic process, that of invasion and angiogenesis. S100A13 is involved in the regulation and release of pro-angiogenic molecules FGF-1 and IL-1 $\alpha$  in a copper-dependent manner.<sup>27,31</sup> Hayrabyan and colleagues also implicated S100A13 as a marker of angiogenesis in endometriosis<sup>32</sup> and used immunohistochemistry to demonstrate that S100A13 was overexpressed in endometriotic tissue, compared to normal endometrium. In 2006, Landriscina and colleagues<sup>27</sup> investigated the expression of S100A13 in human astrocytic gliomas, and reported a positive correlation be-

tween S100A13 expression and both tumour grade and microvessel density. They also propose that in an FGF-1-rich background in low grade tumours, the angiogenic phenotype may be linked to increased S100A13 expression.

It is known that S100 proteins can regulate progression through the cell cycle.<sup>33</sup> We found that decreasing S100A13 expression had no effect on proliferation (Fig. 5) thereby indicating no obvious role for S100A13 in cell growth or apoptosis in these cell lines, although more specific analysis such as H<sup>3</sup>-thymidine incorporation assays and TUNEL assays would clarify this further. This result is in contrast with other findings where limiting S100A13 availability through treatment with the anti-allergic drug Amlexanox resulted in non-apoptotic inhibition of cell migration and proliferation.<sup>34</sup> However, the decrease in proliferation observed in the study may also be attributed to the inhibition of FGF-1 release by Amlexanox and not simply the limited availability of S100A13.

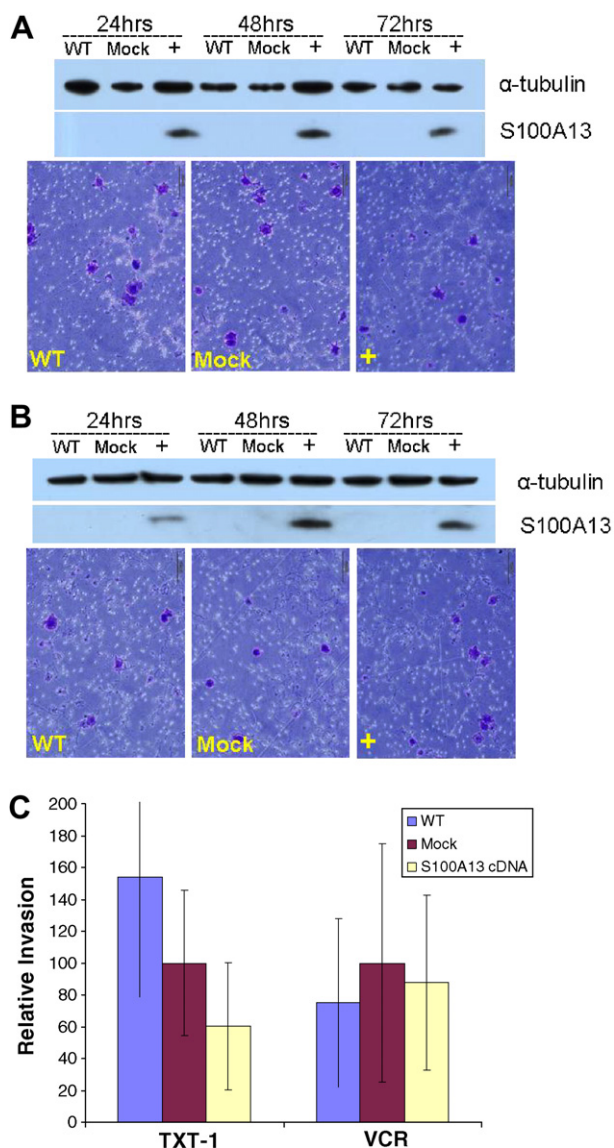


**Fig. 6 – Transient over-expression of exogenous S100A13 had no significant effect on the invasive phenotype in poorly invasive DLKP variants. Western blot with S100A13-specific antibody identified a band at 11 kDa from TX-1 (A) and VCR (B) cell lysates at various timepoints. Invasion assay results represent 72 h post-transfection. WT: untransfected; Mock: empty vector; +: S100A13 expression vector. Large error bar in graph due to very limited number of cells invading (typically 0–12 per field). Data represent counts from 10 fields of view  $\pm$ SD.**

S100A13 cDNA was transiently transfected into the less invasive cell lines TX1 and VCR to determine if an invasive phenotype could be induced. Increased S100A13 expression was confirmed by Western blot however, no effect on invasion was observed indicating that upregulation, at least transiently, is insufficient to transform weakly/non-invasive DLKP cells to a more aggressive phenotype (Fig. 6). In addition, the absence of detectable endogenous protein, despite active transcript expression, may suggest that only very low levels of protein are required to enhance the phenotype in highly

invasive cells – as knockdown with siRNA has a significant impact. These results suggest that S100A13 might act as an enhancer of invasion, given an already invasive background. In this way, S100A13 may act in a similar manner to S100A4, whose expression is also increased in metastatic tumours although transgenic mice overexpressing S100A4 do not develop tumours. S100A4, like S100A13, can be secreted and once extracellular, can also affect angiogenesis.<sup>35</sup> Additionally, extracellular S100A4 can also affect cell differentiation and migration, however, a role for S100A13 has not been reported in these processes at this time.

The results detailed here clearly show S100A13 plays a functional role in invasion as measured *in vitro*. The mechanism by which S100A13 impacts this phenotype remains to be determined, although preliminary indications are that it is not involved in the regulation of cell growth. Further characterisation of the molecular mechanisms by which S100A13 effects both invasion and angiogenesis will aid the understanding of the contribution of S100A13 to the metastatic process and could represent a new target for cancer therapy.

### Conflict of interest statement

None declared.

### Acknowledgements

The authors thank Dr. Padraig Doolan for assistance with Fig. 1; Dr. Patrick Gammell for assistance with siRNA and J. Cahill, Y. Liang for providing cell lines. They also thank Prof. Dr. Claus W. Heizmann (University of Zurich, Switzerland) for providing S100A13 antibody as a kind gift. This work was supported by funding from the Higher Education Authority Program for Research in Third Level Institutions (Cycle 3).

### REFERENCES

1. Santamaria-Kisiel L, Rintala-Dempsey AC, Shaw GS. Calcium-dependent and -independent interactions of the S100 protein family. *Biochem J* 2006;396(2):201–14.
2. Lefranc F, Golzarian J, Chevalier C, et al. Expression of members of the calcium-binding S-100 protein family in a rat model of cerebral basilar artery vasospasm. *J Neurosurg* 2002;97(2):408–15.
3. Bronckart Y, Decaestecker C, Nagy N, et al. Development and progression of malignancy in human colon tissues are correlated with expression of specific Ca(2+)-binding S100 proteins. *Histol Histopathol* 2001;16(3):707–12.
4. Marenholz I, Heizmann CW, Fritz G. S100 proteins in mouse and man: from evolution to function and pathology (including an update of the nomenclature). *Biochem Biophys Res Commun* 2004;322(4):1111–22.
5. Donato R. Intracellular and extracellular roles of S100 proteins. *Microsc Res Tech* 2003;6:540–51.
6. Donato R. S100: A multigenic family of calcium-modulated proteins of the EF-hand type with intracellular and extracellular functional roles. *Int J Biochem Cell Biol* 2001;33:637–68.



7. Heizmann CW, Fritz G, Schafer BW. S100 proteins: Structure, functions and pathology. *Front Biosci* 2002;7:1356–68.
8. Garrett SC, Varney KM, Weber DJ, Bresnick AR. S100A4, a mediator of metastasis. *J Biol Chem*. 2006;281(2):677–80.
9. Rehman I, Cross SS, Catto JW, et al. Promoter hypermethylation of calcium binding proteins S100A6 and S100A2 in human prostate cancer. *Prostate* 2005;65(4):322–30.
10. El-Rifai W, Moskaluk CA, Abdrabbo MK, et al. Gastric cancers overexpress S100A calcium-binding proteins. *Cancer Res* 2002;62(23):6823–6.
11. Kennedy RD, Gorski JJ, Quinn JE, et al. BRCA1 and c-Myc associate to transcriptionally repress psoriasin, a DNA damage-inducible gene. *Cancer Res* 2005;65(22):10265–72.
12. Maelandsmo GM, Florenes VA, Mellingsaeter T, Hovig E, Kerbel RS, Fodstad O. Differential expression patterns of S100A2, S100A4 and S100A6 during progression of human malignant melanoma. *Int J Cancer* 1997;74(4):464–9.
13. Krop I, Marz A, Carlsson H, et al. A putative role for psoriasin in breast tumor progression. *Cancer Res* 2005;65(24):11326–34.
14. Zhang L, Fogg DK, Waisman DM. RNA interference-mediated silencing of the S100A10 gene attenuates plasmin generation and invasiveness of Colo 222 colorectal cancer cells. *J Biol Chem* 2004;279(3):2053–62.
15. Saleem M, Adhami VM, Ahmad N, Gupta S, Mukhtar H. Prognostic significance of metastasis-associated protein S100A4 (Mts1) in prostate cancer progression and chemoprevention regimens in an autochthonous mouse model. *Clin Cancer Res* 2005;11(1):147–53.
16. Wicki R, Schafer BW, Erne P, Heizmann CW. Characterization of the human and mouse cDNAs coding for S100A13, a new member of the S100 protein family. *Biochem Biophys Res Commun* 1996;227(2):594–9.
17. Ridinger K, Schafer BW, Durussel I, Cox JA, Heizmann CW. S100A13. Biochemical characterization and subcellular localization in different cell lines. *J Biol Chem* 2000;275(12):8686–94.
18. Mouta Carreira C, LaVallee TM, Tarantini F, et al. S100A13 is involved in the regulation of fibroblast growth factor-1 and p40 synaptotagmin-1 release in vitro. *J Biol Chem* 1998;273(35):22224–31.
19. Presta M, Dell'Era P, Mitola S, Moroni E, Ronca R, Rusnati M. Fibroblast growth factor/fibroblast growth factor receptor system in angiogenesis. *Cytokine Growth Factor Rev* 2005;16(2):159–78.
20. Folkman J, Shing Y. Angiogenesis. *J Biol Chem* 1992;267(16):10931–10934.
21. Mandinova A, Soldi R, Graziani I, et al. S100A13 mediates the copper-dependent stress-induced release of IL-1alpha from both human U937 and murine NIH 3T3 cells. *J Cell Sci* 2003;116(Pt 13):2687–96.
22. Law E, Gilvarry U, Lynch V, Gregory B, Grant G, Clynes M. Cytogenetic comparison of two poorly differentiated human lung squamous cell carcinoma lines. *Cancer Genet Cytogenet* 1992;59(2):111–8.
23. Rafii S, Lyden D. S100 chemokines mediate bookmarking of premetastatic niches. *Nat Cell Biol* 2006;8(12):1321–3.
24. Stein U, Arlt F, Walther W, et al. The metastasis-associated gene S100A4 is a novel target of beta-catenin/T-cell factor signaling in colon cancer. *Gastroenterology* 2006;131(5):1486–500.
25. Diederichs S, Bulk E, Steffen B, et al. S100 family members and trypsinogens are predictors of distant metastasis and survival in early-stage non-small cell lung cancer. *Cancer Res* 2004;64(16):5564–9.
26. Komatsu K, Murata K, Kameyama M, et al. Expression of S100A6 and S100A4 in matched samples of human colorectal mucosa, primary colorectal adenocarcinomas and liver metastases. *Oncology* 2002;63(2):192–200.
27. Landriscina M, Schinzari G, Di Leonardo G, et al. S100A13, a new marker of angiogenesis in human astrocytic gliomas. *J Neurooncol* 2006;80(3):251–9.
28. Rmali KA, Puntis MC, Jiang WG. Tumour-associated angiogenesis in human colorectal cancer. *Colorectal Dis* 2007;9(1):3–14.
29. Smirnov DA, Zweitzig DR, Foulk BW, et al. Global gene expression profiling of circulating tumor cells. *Cancer Res* 2005;65(12):4993–7.
30. Cristofanilli M, Hayes DF, Budd GT, et al. Circulating tumor cells: a novel prognostic factor for newly diagnosed metastatic breast cancer. *J Clin Oncol* 2005;23(7):1420–30.
31. Landriscina M, Bagala C, Mandinova A, et al. Copper induces the assembly of a multiprotein aggregate implicated in the release of fibroblast growth factor 1 in response to stress. *J Biol Chem* 2001;276(27):25549–57.
32. Hayrabedyan S, Kyurkchiev S, Kehayov I. Endoglin (cd105) and S100A13 as markers of active angiogenesis in endometriosis. *Reprod Biol* 2005;5(1):51–67.
33. Breen EC, Tang K. Calcyclin (S100A6) regulates pulmonary fibroblast proliferation, morphology, and cytoskeletal organization in vitro. *J Cell Biochem* 2003;88(4):848–54.
34. Landriscina M, Prudovsky I, Mouta Carreira C, Soldi R, Tarantini F, Maciag T. Amlexanox reversibly inhibits cell migration and proliferation and induces the Src-dependent disassembly of actin stress fibers in vitro. *J Biol Chem* 2000;275(42):32753–62.
35. Kim EJ, Helfman DM. Characterization of the metastasis-associated protein, S100A4. Roles of calcium binding and dimerization in cellular localization and interaction with myosin. *J Biol Chem* 2003;278(32):30063–73.